

Applicability of over-coring technique to loaded RC columns

Giuseppe Campione^{*1} and Giovanni Minafò^{2a}

¹Dipartimento di Ingegneria Civile Ambientale Aerospaziale e dei Materiali DICAM, Università di Palermo,
Viale delle Scienze, 90128 Palermo, Italy

²University "Kore" of Enna, Faculty of Engineering and Architecture, Cittadella Universitaria, 94100 Enna, Italy

(Received June 13, 2012, Revised May 9, 2014, Accepted May 17, 2014)

Abstract. Stress determination is a very important step in the assessment of the safety of existing reinforced concrete structures. In rock mechanics this goal is achieved with the over-coring technique. The main idea behind such a technique is to isolate a material sample from the stress field in the surrounding mass and monitor its re-equilibrium deformation response. If the materials remains elastic, and elastic properties are known, stresses may be obtained from the corresponding measured strains. The goal of this paper is to evaluate if the over-coring technique is applicable to reinforced concrete members. The results of an experimental investigation on the behaviour of compressed concrete columns subjected to the over-coring technique are presented. Considerations about the range of applicability of the technique are made by comparing the measured and the theoretical stresses. After that, results of failure tests on drilled specimens are presented and discussed. Furthermore, the response is compared with that of columns core-bored before the compressive test. Finally, comparisons with numerical analysis are shown.

Keywords: experimental research; over-coring technique, RC columns; compressive tests; reduction of bearing capacity

1. Introduction

Nondestructive testing (see e.g., ACI 228.1R, ACI 214.4R, BS1881-120, 43-CND) today is becoming of fundamental importance for a checkup on the structure, also in the field of civil and infrastructure engineering.

Among testing modalities the over-coring technique, which is a well-known experimental method in rock mechanics (Leite *et al.* 2010) is also performed for determination of in-situ stress in concrete dams, bridges and viaducts. The basic principle of this method is measurement of the variation in the strain state due to the removal of a part of material by core drilling. The over-coring technique can be summarized in the following points: a cylindrical core is gradually isolated in advancing steps using a diamond core drill bit, in a perpendicular direction to the external surface. At every step, the strain gages, placed on the core external surface, indirectly measure the gradual stress release on the core edge (see Fig. 1). Finally, the original stress state is calculated on the basis of recorded strains, knowing the elastic characteristics of the material

*Corresponding author, Associate Professor, E-mail: studioingcampione@libero.it

^aPost-doctoral Researcher, E-mail: giovanni.minafo@unikore.it

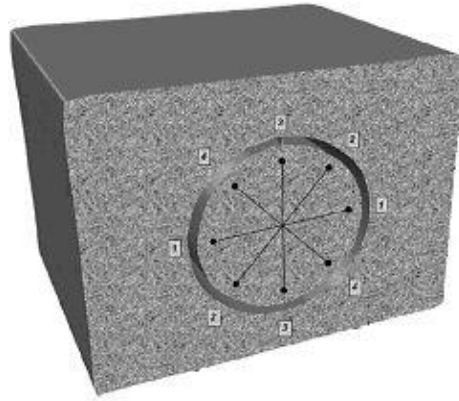


Fig. 1 Pattern of a surface over-coring test

deduced e.g., from compressive tests on the extracted cylindrical core. The data on the stress state obtained with the surface over-coring technique are very important, not only for a direct check on the values of internal forces, but also (and perhaps above all) for validation and calibration of numerical models usually adopted in structural analysis. With such a technique, the complete stress tensor can be obtained with most strain gages devices, also determining the mechanical characteristic from the extracted core.

The method is similar to the American Society for Testing and Materials (ASTM) hole-drilling strain gage method (ASTM 837 2008), suitable to determine residual stresses in homogenous materials such as metals. The ASTM hole-drilling strain gage method⁰ has been the subject of numerous technical publications, including methods to reduce the dependence of the calculations on material properties, to refine the techniques involved for calculation of non-uniform stresses through depth and utilize the advantages of finite element analysis, and to apply the technique to orthotropic materials.

Barrallo *et al.* (1999) proposed to apply the technique to ancient masonry structures by modifying the test set-up provided in ASTM 837 (2008). Sanchez-Beitia (2007, 2008) afterwards presented different applications of the proposed technique to existing masonry structures, showing that in such cases the technique could be reliably applied. The first application of the technique in concrete structures was proposed by McGinnis *et al.* (2005).

The authors modified the technique applied in steel members, by considering displacements rather than strains and performing measurements with photogrammetry and by means of a three-dimensional digital image correlation.

They also validated the method with laboratory tests carried-out on steel plates. Trautner *et al.* (2011) recently extended the same technique to prestressed concrete beams, correlating the recorded displacements with the in-situ stresses by means of influence function coefficients.

Although the adaptation of the over-coring technique to actual structures is of great practical interest, at the authors best knowledge a few of experimental investigations were carried-out on axially-loaded RC members. In such case some disadvantages have been encountered in the application of the over-coring technique, as documented from application of over-coring in mining engineering (Coetzer 1997): - epoxy based adhesives are not suitable for use in dirty, wet or humid environments, which can be a problem for existing structures in aggressive environments; - strain

gages require specialized installation techniques ensuring that they are directly bonded to the core surface and are not easily damaged; - micro cracking can occur, damaging the strain gages; - measurements can be affected by the size of coarse aggregate.

It has to be reminded that in engineering practice, it is strongly discouraged to take core samples from columns, due to the damage induced by the hole in the member. In cases where it is unavoidable, strict rules concerning the size and location of the cores apply. Previous studies had experimentally evaluated the reduction of load-carrying capacity due to core drilling. Zhu *et al.* (2010) performed compressive tests on nine drilled RC columns and found reductions of axial compressive strength up to 22%. Analogously, Campione and Minafò (2011) tested eight columns with different reinforcement arrangements and hole locations. The authors found strength reductions of about 30% and proposed a simplified analytical model to evaluate the splitting failure load of such members. Consequently the proposed technique could cause damage in some case. For these reasons, additionally to the over-coring tests, also compressive failure tests were performed on plain and RC columns. Considerations about the reduction of load-carrying capacity were made and experimental results were compared with analytical predictions.

2. Research significance

Currently no test can be performed on reinforced concrete (RC) structures to know the stress state (as can be made in masonry structures by flat-jacks technique (ASTM C 1196)). Hence the adaptation of the over-coring technique to RC structures can be very useful, both for stress control in members that have to be retrofitted and for calibration of numerical models generally adopted in structural analysis. This paper presents test results of 8 short columns subjected to the over-coring technique. Considerations about the range of applicability of the technique are made on the basis of the load level. Compressive failure tests on over-cored members and on drilled columns (cored before testing) are also performed and results are discussed and compared. The loss of load-carrying capacity due to the hole is measured, as already done in Campione and Minafò (2011). The results are discussed and compared with finite element analysis carried out with ATENA software (Cervenka 2000).

3. Experimental programme

Surface over-coring tests were performed on RC columns; the specimens were cast in a laboratory and subjected to a vertical fixed load, which was kept constant during the test with a machine press. During the tests, the strains were recorded on the edge of the hole, and the corresponding stresses were calculated from these by means of the elastic theory (knowing the elastic properties of the concrete). The stresses obtained in this way were compared with those obtained theoretically, induced by the axial load.

Core boring was performed on a member that was artificially loaded, in order to reproduce, as well as possible, the stress state in a compressed column of a RC structure.

Furthermore, another object of the experimental program was the evaluation of the influence of a hole on the load-carrying and deformation capacity of compressed columns in reinforced or plain concrete.

Table 1 Characteristics of tested specimens

No. of columns	Reinforcement		Over-coring test		Compressive test to failure	
	Longitudinal bars	Stirrups	No. of columns	Applied load (percentage of failure load)	Solid	Drilled
2	/		1	20%	1	1
2	4 Φ 12 mm	6 Φ 6 mm	1	20%	1	1
2	/		1	40%		
2	4 Φ 12 mm	6 Φ 6 mm	1	40%		

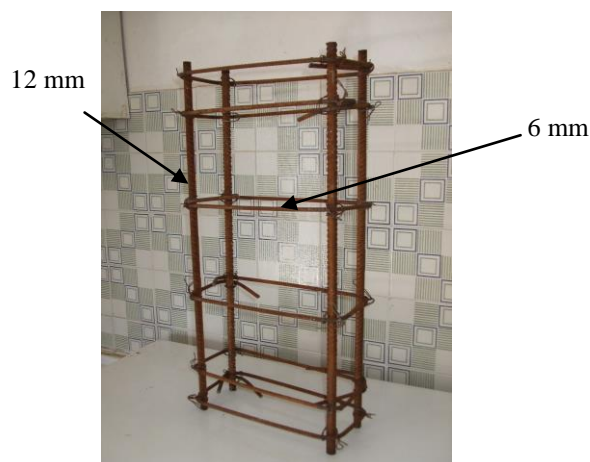


Fig. 2 Geometry of specimens and reinforcement cage (unit: mm; 1 mm = 0.039 in)

Specimen details

The main features of the specimens cast are reported in Table 1. The columns had a rectangular cross-section of width 300 mm and depth 150 mm and height 600 mm. It has to be noted that from St. Venant's principle the total extent of the disturbed region (along the specimen height) about the hole has to be equal to twice the panel width plus the diameter of the hole (Campione and Minafò 2011). For a hole diameter of 100 mm and panel width of 300 mm the panel height should be at least 700 mm. It was assumed equal to 600 mm (23.4 mm) due to the limitations of the testing machine. Further investigations will be addressed to evaluate these effects. Reinforcements consisted in four deformed 12 mm longitudinal bars placed at the corners and 6 mm stirrups spaced at 150 mm (see Fig. 2).

The clear concrete cover was 20 mm. Furthermore, the heads of the specimens were additionally reinforced with three steel stirrups spaced at 50 mm for both heads.

The top and bottom surfaces of specimens were levelled with a thickness of 20 mm of high-strength mortar in order to have planar and parallel surfaces. The geometrical ratio of the longitudinal bars was $\rho = A_s / (b x h) = 1\%$, while that for stirrups in the pitch p was $\rho_{sw} = A_{sw} / (p x h) = 0.13\%$. Such low values of geometrical ratio of reinforcement were considered to simulate existing structural members, relative to old buildings designed without seismic provisions. Furthermore the value of ρ_{sw} was assumed less than the limit specified in Section 10.9

Table 2 Mix design and mechanical properties of concrete

Mix design	kg/m ³	Mechanical properties (MPa)	
Cement	350	f'_c	R_c
Water	180	13.96	17.87
Sand	800		
Aggregate (max. side 20 mm)	1100		

Table 3 Mechanical properties of steel bars

Diameter (mm)	f_y (MPa)	f_u (MPa)	ϵ_u (%)
12	476	546	27.5
6	478	569	26.0

of ACI 318-08 code, in order to minimize the confinement effect in the column and also to simulate columns which have to be retrofitted.

Four columns, of the total of eight, two in reinforced concrete and two in plain concrete, were subjected with a force-controlled press machine to a percentage of the theoretical ultimate load equal to 20% and 40%, were over-cored at this load level, and afterwards tested to failure. Four other specimens were core-bored while unloaded and afterwards tested in compression up to failure.

Material characteristics

Specimens were cast with Portland cement 32.5 MPa with water/cement ratio equal to 0.55 and mix design summarized in Table 2. Compressive tests on four 100×200 mm standard concrete cylinders (5.6.3.2 of ACI 318-08) and four 150 mm cubes were undertaken to obtain the compressive strength. The concrete at 28 days exhibited average values of cube R_c and cylinder f'_c compressive strength, as shown in Table 2. Tensile tests on reinforcing deformed bars of diameter 6 and 12 mm were performed to obtain the complete stress-strain curve in tension, not shown for brevity sake; the results are summarized in Table 3, where f_y is the yield stress, f_u is the ultimate stress and ϵ_u is the ultimate strain.

Test set-up

Tests were conducted in two distinct phases: the first phase was relative to the over-coring test, where the specimen was loaded with a fixed load level; the second phase included compressive tests to failure on totally drilled specimens. Over-coring tests were performed with core boring advancing in steps of 20 mm and simultaneously measuring the strains at the edge of the hole by means of strain gages. The strains assumed for the determination of stresses were the stabilized ones; to be more precise, these were the strains recorded after a time interval, when they can be assumed constant; this could represent an equilibrium index. After the final step (completely drilled) every specimen was tested to failure.

Fig. 3 shows the phases of the over-coring test: (a) the specimen was loaded, with a press machine, up to a fixed load level (20% or 40% of the ultimate load), Fig. 3(a), (b) while keeping this load level constant, the specimen was core-bored, Fig. 3(b), and (c) the load was increased until failure, Fig. 3(c).

Core-boring was achieved by a Hilti DD250E rotary drilling machine with a diamond core drill

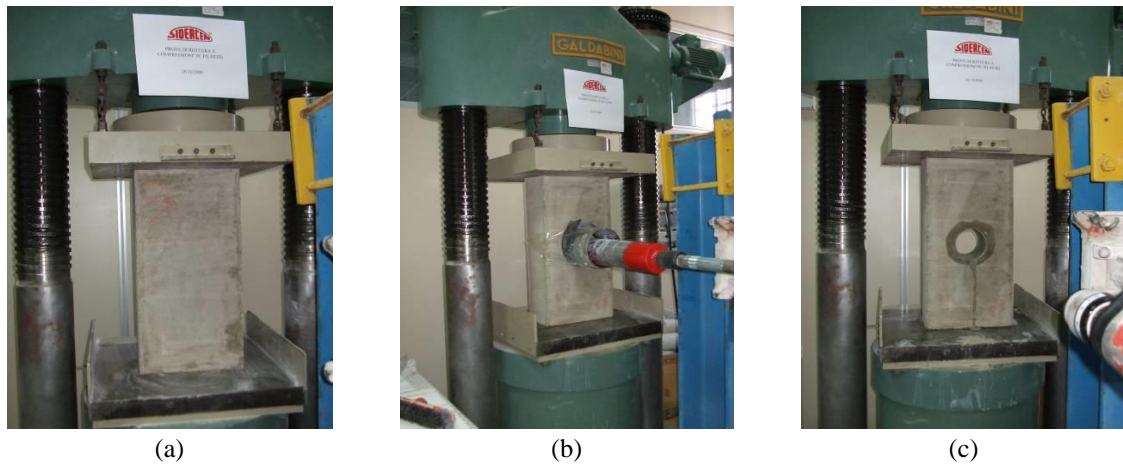
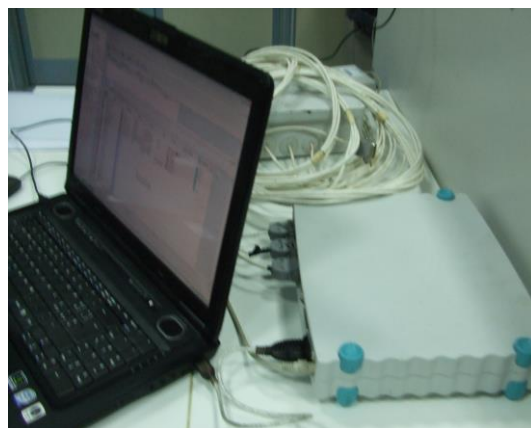


Fig. 3 Column over-cored under a fixed load; (a) Solid specimen under a fixed load; (b) Core-boring phase; (c) Completely drilled specimen



(a)



(b)

Fig. 4 Measuring system (a) PC and measurement unit; (b) Strain gages mounted on the core surface

bit of diameter 100 mm (3.9 in) and variable depth during the test. HBM LY41-50/120 strain gages were mounted on the front side (the side that had to be drilled). Data recording was done with the HBM Spider8 multi-channel electronic PC measurement unit and the Catman Professional 5.0 software (Fig. 4(a)). Strain gages had a gage length of 70 mm and were placed horizontally, vertically and with a slope of 45° , as shown in Fig. 4(b). After the specimen was placed under the bearing plates of the press machine, it was loaded with fixed load levels (20% and 40% of the theoretical ultimate load) and afterwards it was gradually core-bored with advancing steps of 20 mm (0.78 in) and before the following step, waiting for a long enough time to allow stabilization of the strain gage readings (meaning a constant value of the measured strains).

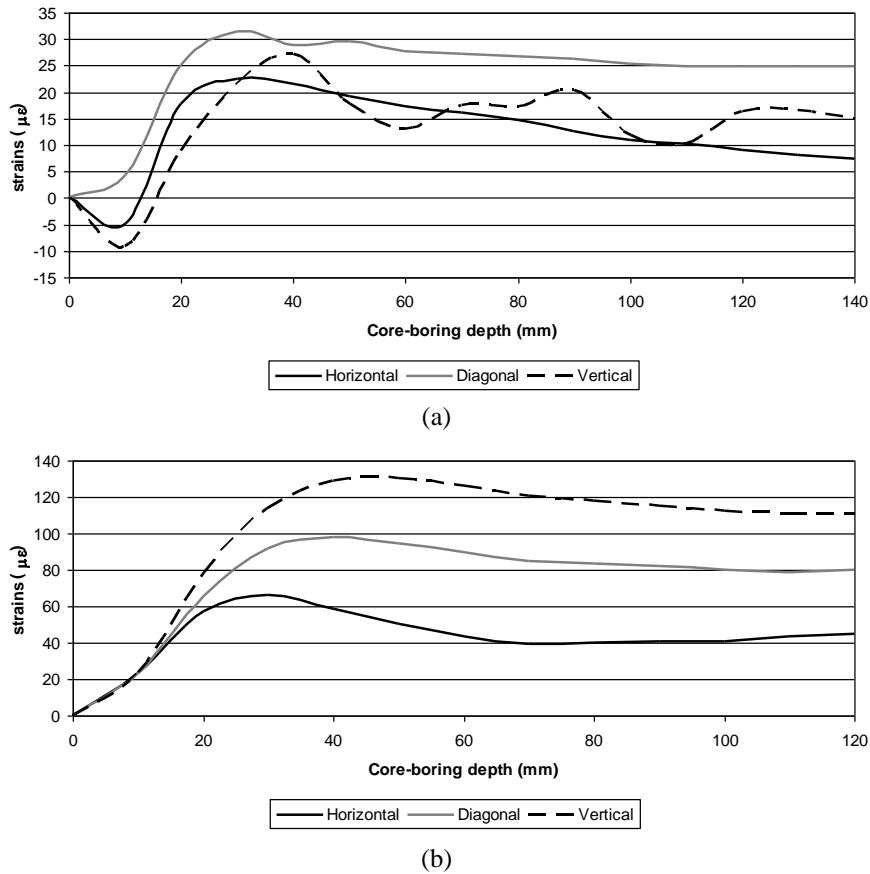


Fig. 5 Trend of strains with depth of core boring; (a) Specimen loaded with 20% of theoretical ultimate load; (b) Specimen loaded with 40% of the theoretical ultimate load. (unit: mm; 1 mm = 0.039 in)

A measurement system allowed strain recording on the surface of the cylindrical core and knowing the elastic modulus and the Poisson's coefficient the stresses could be computed and compared with those acting in the column.

4. Experimental results

In this section, the results of superficial over-coring tests performed in RC and plain concrete specimens are presented. Furthermore the results of compressive failure tests on over-cored columns are presented and compared with those relative to drilled columns, which were not subjected to the over-coring.

Over-coring test results

Two RC specimens and two plain concrete specimens were axially-loaded in compression with a fixed load level equal to 20% and 40% of the ultimate load computed theoretically on the basis of the compressive strength of the concrete and of the yield strength of steel rebar. These load

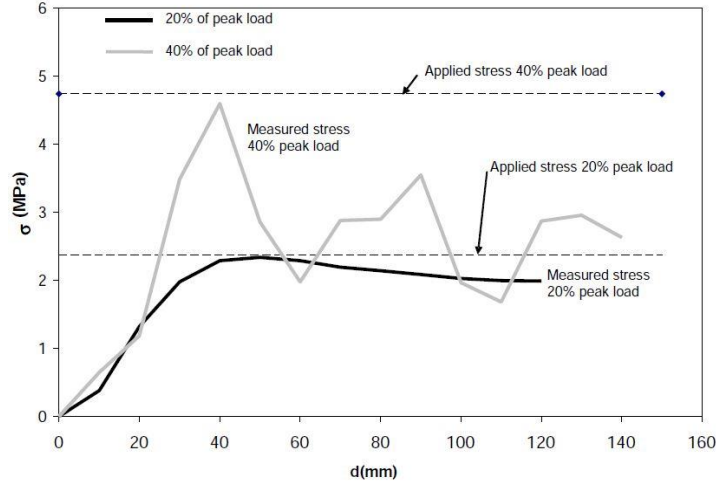


Fig. 6 Trend of axial stress with core boring depth (unit: mm; 1 mm=0.039 in, 1 lb/ in²=0.00703 MPa)

levels were chosen to reproduce the stress state in a column during the service condition and during the non-linear behaviour of the column, which is far enough from the theoretical failure load value.

Fig. 5 shows the axial, horizontal and diagonal strain near the hole as a function of the depth of the core-boring. Specifically, Fig. 5 (a) and (b) are relative to specimens loaded respectively with a load level of 20% and 40% of the ultimate theoretical load with respect to the case of an RC column.

The axial strain near the edge of the hole increases with the core boring depth until it takes on a quasi-constant value when the specimen is completely drilled; this represents an index of the new equilibrium of the internal forces in the specimen.

Fig. 6 shows the trend of the axial stress with the core boring depth for plain concrete specimens. The axial stresses were computed with the fundamental expressions of the elasticity theory listed below

$$\begin{aligned}\sigma_{xx} &= \frac{E_{cm}}{(1-\nu^2)}(\varepsilon_x + \nu\varepsilon_y) \\ \sigma_{yy} &= \frac{E_{cm}}{(1-\nu^2)}(\varepsilon_y + \nu\varepsilon_x)\end{aligned}\quad (1)$$

where ε_x and ε_y are respectively the vertical and the horizontal strains and ν is the Poisson's coefficient, assumed equal to 0.15.

In the considered case, the elasticity modulus for concrete E_{cm} , was calculated neglecting the effect of time and temperature; it can be computed according to the relation suggested in Eurocode 2

$$E_{cm} = 22000 \cdot \left(\frac{f_{cm}}{10}\right)^{0.3} \quad (\text{MPa}) \quad (2)$$

or according to the expression provided in ACI 318-08¹⁰

$$E_{cm} = 4730\sqrt{f_{cm}} \text{ (MPa)} \quad E_{cm} = 57,000\sqrt{f_{cm}} \text{ (psi)} \quad (3)$$

where f_{cm} is the average cylinder compressive strength of the concrete.

It has to be reminded that for existing structures the long-term effects has to be taken into account and consequently the variations of elastic modulus and compressive strength of concrete have to be considered. Eurocode 2 with reference to a standard temperature of 20°C suggested the following expression to calculate the value of the compressive strength at a time t (expressed in number of days)

$$f_{cm}(t) = \beta_{cc}(t) \cdot f_{cm} \quad (4)$$

where $\beta_{cc}(t)$ was a function of the time t and can be evaluated as: $\beta_{cc}(t) = e^{s \left[1 - \left(\frac{28}{t} \right)^{1/2} \right]}$

while s was a coefficient which depend on the cement strength and can be assumed as 0.2 for high strength cement, 0.25 for normal strength cement and 0.38 for low-hardening cement.

The elastic modulus of concrete $E_{cm}(t)$ at time t can be calculated with the expression proposed from the same code

$$E_{cm}(t) = \left(\frac{f_{cm}(t)}{f_{cm}} \right)^{0.3} \cdot E_{cm} \quad (5)$$

It can be observed that for a load level of 20% of the ultimate load and in the absence of a hole, the elasticity theory makes it possible to calculate a stress in the vertical direction that tends to be constant and to approach the actual stress in the vertical direction (dashed line in Fig. 6).

By contrast, for a load level of 40% of the ultimate load, the elasticity theory leads to a substantial difference between the value of the vertical stress and the effectively acting stress.

This is due to the fact that, for such a load level, the intensification of stresses near the hole leads to strong non-linear behaviour that causes the difference between the stresses deduced with the elasticity theory and those effectively acting. Consequently, it can be observed that the over-coring technique can be performed with acceptable results only if the structure is in the elastic phase during the test and if the perturbation due to core boring only causes a local effect and does not influence the overall behaviour of the member.

The case examined here could represent a short column with a standard cylindrical hole due to concrete drilling.

Failure test results

Fig. 7 shows the stress-strain curves for the plain concrete columns. In particular the results of the solid and over-cored specimens tested to failure are shown. From Fig. 7 it clearly emerges that stiffness results are similar for the solid and over-cored columns up to 20% load level, and significantly different at 40% load level.

After over-coring, the stiffness decreased and the specimen showed strong non-linear behaviour until the peak was reached. The load-carrying capacity of drilled columns was always lower than that of solid specimens and the greatest reduction occurred for specimens that were preliminarily drilled. The presence of the hole caused a load-carrying capacity reduction of about 20%, which was a value lower than the reduction in the area of the cross section (33%). Another consequence due to the presence of the hole was the reduction in the overall deformability of the drilled

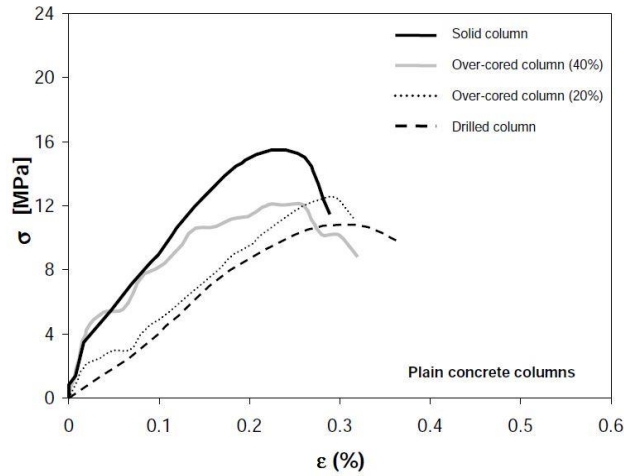


Fig. 7 Compressive tests on plain concrete columns ($1 \text{ lb/in}^2 = 0.00703 \text{ MPa}$)

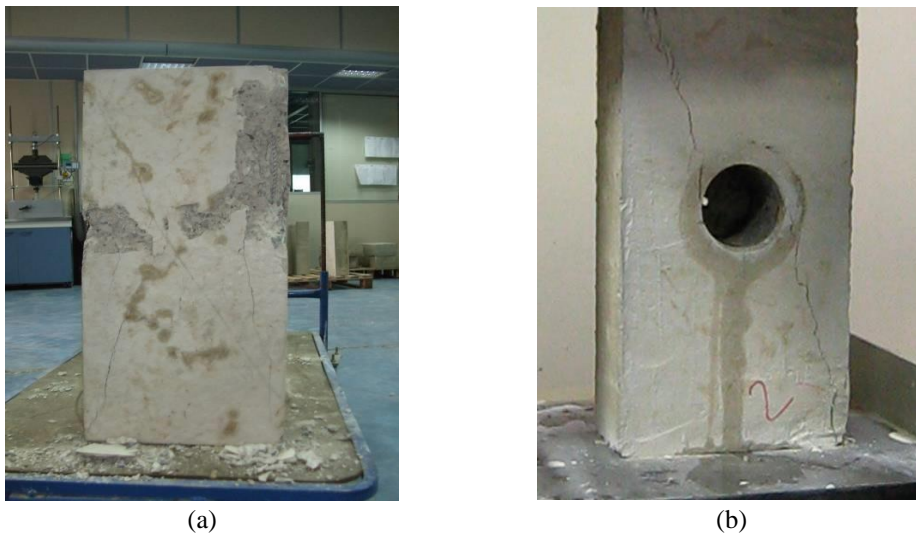


Fig. 8 Failure modes of plain concrete specimens (a) solid specimen; (b) drilled specimen

member. After the maximum strength was reached, all the specimens showed a softening phase with the failure modes shown in Fig. 8(a) for solid specimens and Fig. 8(b) for drilled specimens. Classical crack patterns could be observed for both solid and drilled columns. For the latter, this was characterized though diagonal cracks starting from the top and bottom ends of the column and propagating toward the hole in a position that was roughly diametrically opposite.

Fig. 9 shows the concrete stress vs. axial strain curves for the RC columns. In this case too, the results for solid specimens tested to failure, over-cored specimens and preliminarily drilled specimens afterwards tested to failure are reported. The presence of the hole caused a reduction of about 30% in load-carrying capacity, which was a similar value to the reduction of the cross-section (33%).

The peak strain was greater than for plain concrete specimens. The failure modes are shown in

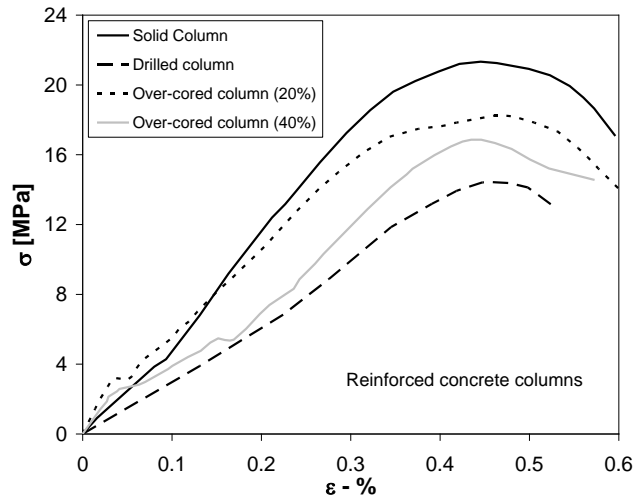


Fig. 9 Compressive tests on reinforced concrete columns ($1 \text{ lb/in}^2 = 0.00703 \text{ MPa}$)

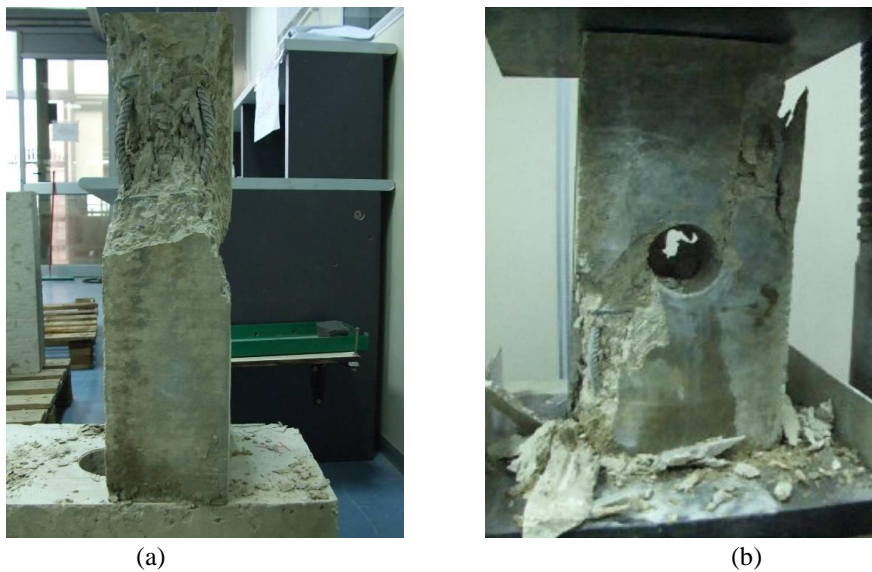


Fig. 10 Failure modes of reinforced concrete specimens (a) solid specimen; (b) drilled specimen

Fig. 10(a) for solid specimens and Fig. 10(b) for drilled specimens. The crack pattern is similar to that described before for plain concrete specimens, with diagonal and symmetrical cracks joining in the hole. For the solid specimens, the main cracks were in the vertical direction, and in particular were concentrated in the top ends of the front and the side faces.

5. Analytical interpretation of experimental results

In order to obtain a numerical prediction of load-carrying capacity of tested specimens, a non-

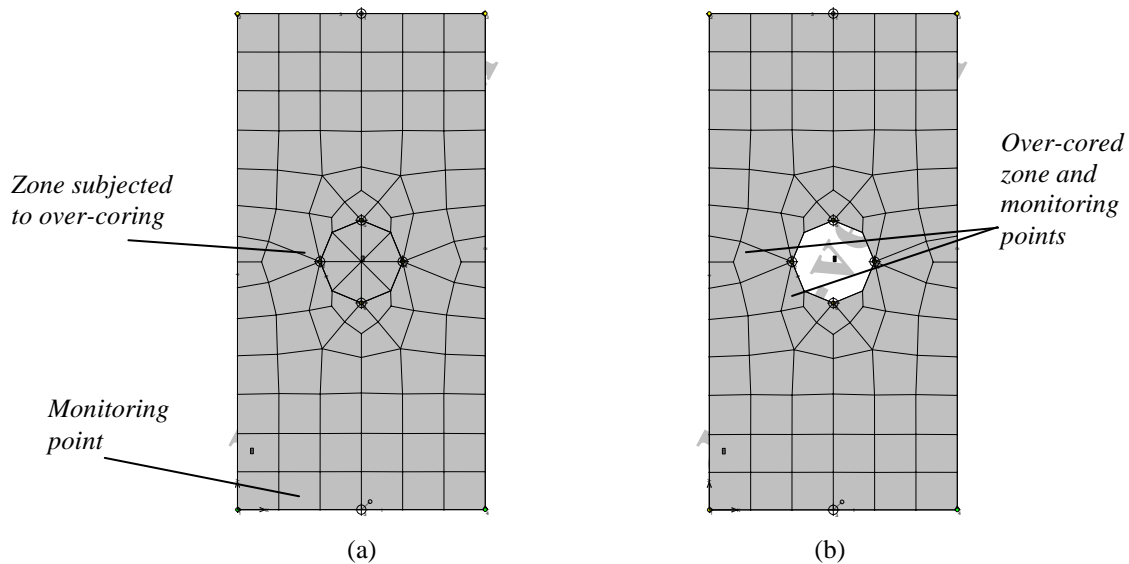


Fig. 11 Finite element model: (a) undrilled Specimen (b) Drilled specimen

linear finite element analysis was carried out using the ATENA2D commercial program (Cervenka 2000). This software was used because it allows complete modelling of RC structures and is today utilised by practicing engineers for non-linear behaviour of RC structures. The concrete was modelled using nine-node isoparametric shell elements, while discrete bars were used to model the reinforcements (longitudinal bars and transverse stirrups).

The “SBeta” constitutive law of concrete in compression, including softening and damage, was assumed; while in tension the linear stress-strain relationship was assumed until tensile strength was reached, afterwards assuming an exponential crack opening law by means of fracture energy. The constitutive laws adopted were calibrated on the basis of the experimental results. An elastic-plastic constitutive law was assumed for steel reinforcements in both compression and tension.

A typical model adopted for solid and cored specimens is shown in Fig. 11.

Simulation of over-coring tests

The analysis was carried out on different finite element models, able to reproduce the displacement controlled test by imposing incremental steps of 0.05 mm (0.0195 in). All the models were calibrated in order to include the presence of a cylindrical hole in the centre of the specimen and the arrangement of longitudinal bars and stirrups, if any. The models had varying thickness in the drilling zone, ranging from total specimen thickness (representing the initial stage) to zero (completely drilled specimen), to simulate the over-coring test with advancing coring steps. For every value of coring depth the total response was recorded.

The strains recorded from the numerical model on the edge of the hole and on the total length of the specimens (shortening) were compared with those recorded during the test. Considering the shortenings and the vertical stresses measured on the total specimen length, the difference between the numerical and the experimental value was represented in Fig. 12 in graph form. In this figure the difference between numerical and experimental values represents the error and its value is shown in the ordinate axis, while the load level is represented in the abscissa axis. From the results

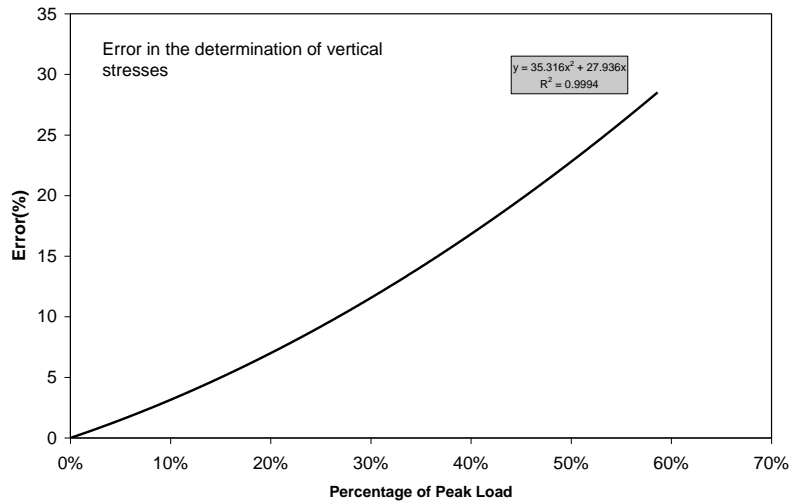


Fig. 12 Variation in error in determination of vertical stresses with percentage of peak load

obtained it emerges that the accuracy of the test decreases when the load level increases, due to the ending of the elastic phase of the concrete as observed experimentally. This highlights the fact that the reliability of the test depends on the behaviour of the structure, which should be elastic; therefore it is advisable to perform the over-coring test with other complementary tests that ensure the elastic nature of the problem.

The trend of the error with the load level was approximated with a quadratic law, and from this it clearly emerges that acceptable error values (<15%) can be obtained for load values up to 30-35% of the ultimate load; over these values, the error quickly increases. Furthermore it has to be observed that the strain measurement is affected from different parameters (e.g., fracture impact during drilling, gluing of strain gauges and so on), which contribute to increase difference between measurement and simulation. Therefore quality of the test depends on how these technical problems are solved.

Analysis of reduction in load-carrying capacity due to core-boring

Numerical analysis allows investigation of the variations in strain and stress state on the concrete and on the reinforcing bars due to core-boring.

Fig. 13 shows the trend of the load-carrying capacity. In this figure, the depth of core-boring is reported in the abscissa axis while the maximum vertical stress recorded in a zone far from the hole is reported in the ordinate axis. In the same graph the results of the numerical analysis are reported with a continuous line.

From Fig. 13 it clearly emerges that the increase in core-boring action causes a progressive reduction in load-carrying capacity. From the trend of the results, it clearly emerges that the numerical analysis accurately provides the reduction in load-carrying capacity due to the core-boring action.

Fig. 14 shows the crack pattern at failure obtained with ATENA2D. Specifically, the graphs in Fig. 14(a) refer to plain concrete specimens, while those in Fig. 14(b) refer to RC specimens.

An increase in local deformability near the hole during the loading process is observed, both longitudinal and transverse, corresponding to the distortion of the hole.

From the results of the analysis, it can be observed that reinforcing bars still behaved in an elastic manner when the peak stress of the specimens was reached, because the yielding values of strain and stress (0.23% and 476 MPa (69020 psi)) were not reached.

Furthermore, another consideration concerns the influence of core-boring actions on the stress state of reinforcements: failure of the specimen always occurred for a stress value in the longitudinal bars that decreased when the depth of core-boring increased, while the stress in transverse steel increased. Consequently, core-boring actions are very influential above all for transverse reinforcements near the hole and for longitudinal bars linking them.

Damaging effect of core drilling

In engineering practice, core samples are usually taken to determine the concrete strength. However, it is strongly discouraged to take core samples from columns due to the damage induced by the hole in the member. Nevertheless, it is often unavoidable when existing columns have to be checked or monitored for retrofitting purposes. In such cases, the geometrical discontinuity introduced by core drilling caused a complex stress state, where the classical Bernoulli hypothesis could not be applied. The extent of the disturbed region (D-region) was defined from St.Venant's principle as described above. A bursting tensile force will developed in orthogonal direction to the axis of the column, due to the compressive stress trajectories. If no sufficient transverse reinforcement was provided, a brittle failure occurred due to the low tensile strength of concrete (splitting failure). Consequently the ultimate load depended on concrete strength, transverse reinforcement arrangement and on the dimensions and locations of the hole. Campione and Minafò⁰ had recently proposed an analytical relationship between the axial load and the bursting tensile force, derived by considering an approximate polynomial function describing the isostatic lines of compression

$$C = \frac{128}{15} \cdot T_s \cdot \left(\frac{b}{d} \right) \quad (6)$$

where b was the half-side of the member and d was the diameter of hole.

The expression of T_s depended on the considered failure mode; for the case of splitting failure, a triangular distribution of the transverse tensile stresses could be assumed as experimentally determined by Sahoo *et al.*; consequently, considering the presence of the hole the bursting tensile force can be written as

$$T_{\text{split}} = \left(2b - \frac{d}{2} \right) \cdot t \cdot f_{ct} \quad (7)$$

where t was the thickness of the member and f_{ct} the tensile strength of concrete. If yielding of transverse reinforcement was considered, the bursting tensile force coincided with the yielding force of the stirrups.

$$T_{y,s} = A_{st} \cdot f_y \quad (8)$$

Fig. 15 shows the load-carrying capacity reduction with respect to the theoretical ultimate load for considered specimens, as a function of the core diameter-to-column side ratio. Two different curves could be observed for RC members: the first relative to splitting failure was derived by using Eq. (6) with Eq. (7), while the second was computed by considering Eq. (6) together with Eq. (8). In such a way, for a fixed core diameter-to-column side ratio, a range of load-carrying

capacity reductions could be individuated. Furthermore it has to be noted that for plain concrete specimens, a minor reduction was observed; this is due to the fact that splitting failure load depended only from the tensile strength of concrete while axial capacity of the member was lower due to the absence of longitudinal reinforcement. For considered test specimens ($d/2b=0.33$), the expected axial capacity reduction was in the range between 20% and 40%, as confirmed experimentally. It clearly emerges that for core diameter-to-side of column ratios less than 0.2, no reduction occurred, highlighting the importance in developing micro-core techniques for non-destructive testing.

In similar way the maximum allowable core diameter could be obtained simply by setting Eq. (6) equal to the axial load capacity of the member. In such a way, two relationship of the maximum allowable core diameter could be obtained

$$d_{\max,s} = \frac{1792 \cdot b^2 \cdot \sqrt{f_c} \cdot t}{375 \cdot (2b \cdot t \cdot f_c - A_f \cdot f_{yd}) + 448 \cdot b \cdot \sqrt{f_c} \cdot t} \quad (9)$$

$$d_{\max,y} = \frac{8.53 \cdot b \cdot A_{st} \cdot f_{ys}}{(2b \cdot t \cdot f_c - A_f f_{yl})} \quad (10)$$

Eq. (9) and Eq. (10) were graphically represented in Fig. 16 in non-dimensional form with respect to the column side $2b$, as a function of the geometrical ratio of longitudinal reinforcement ρ_l and for fixed mechanical properties of materials ($f_c=20$ MPa and $f_y=450$ MPa). Also the line corresponding to the minimum values of ρ_l provided from the European and American codes were reported. It is clearly evident from the graph as the core diameter could be increased on the basis of the reinforcement arranged in the column. It has to be noted that for common existing structures with low values of ρ_l (about 1%) and without enough stirrups ($0.1\% < \rho_{st} < 0.2\%$) the core diameter should be limited to the 20% of the column side. By contrast, it is well-known that it is difficult to determine the concrete compressive strength with small-scale specimens. Consequently it could be concluded that core-drilling should be performed in large columns, after a preliminary assessment of the mechanical characteristics and of reinforcement arrangement. However, some aspects here neglected for the sake of simplicity (long-term effects, eccentric location of the hole, repairing of the hole), should be investigated with further experimental and analytical developments.

Applicability and limitations of the over-coring technique for RC members

As stressed before and as confirmed from the experimental results, the applicability of the over-coring technique is strongly related to the linear behaviour of the concrete. Consequently the method can be applied in RC structures but with limitations involving the load levels, the concrete grade and the adopted technical solutions.

For low load levels the over-coring technique can be reliably used for the stress measurement during the elastic phase, while for high load levels, the strictly non-linear behaviour of concrete and the intensification of stresses on the edge of the hole falsify measurements of the stress state. Consequently a preliminary assessment of the service load on the considered column is always necessary to evaluate if the technique is applicable or not.

Furthermore, for a correct application of the over-coring technique, it is of fundamental importance to know of the elastic properties of concrete, which are time-dependent values, as well documented in the literature. Long-term effects have to be taken into account e.g., by considering

the expressions proposed in the codes (Eqs. (4) and (5)). However further experimental investigations have to be addressed on this field.

Also the concrete grade could influence the reliability of the technique. In fact it is well-known that higher-strength concretes display a more linear behaviour to a higher stress-to-strength ratio as compared to normal-(or low-) strength concrete; consequently the accuracy of the method should increase with the concrete strength. For this reason, it is recommend to estimate the concrete strength before performing the over-coring test e.g., with non-destructive testing techniques. Also this important aspect has to be clarified by further experimental investigations.

6. Conclusions

The goal of this paper was to evaluate the applicability of the over-coring technique in evaluating the actual stress in RC columns. From the results obtained in this introductory study, the following considerations can be drawn:

- the method can be applied in RC structures but with limitations involving the load levels, the concrete grade and the adopted technical solutions;
- for a load level of 20% of ultimate load, differences between the actual and the measured stress up to 10% were recorded. Consequently the over-coring technique can be reliably used for the stress measurement for low load levels;
- for high load levels, the strictly non-linear behaviour of concrete and the intensification of stresses on the edge of the hole falsify measurements of the stress state.
- the elastic properties of concrete are time-dependent values. Long-term effects have to be taken into account e.g. by considering the expressions proposed in the codes. However further experimental investigation have to be addressed on this field;
- Concrete grade and long term effects are important aspect which could influence the reliability of the technique. Further experimental investigations have to be addressed in these fields.

References

- ACI 228.1R-03 (2003), "In-place methods for determination of strength of concrete", *ACI Mater. J.*, **85**(5), 446-471.
- ACI 214.4R (2008), "Guide for obtaining cores and interpreting compressive strength results", Detroit, Michigan.
- British Standards Institution (1981), "BS 6089: Guide to Assessment of Concrete Strength in Existing Structures", London W4 4AL, United Kingdom.
- RILEM Draft Recommendation 43-CND (1993), "Combined non-destructive testing of concrete - Draft recommendation for in situ concrete strength determination by combined non destructive methods", *Mater. Struct.*, **26**, 43-49.
- Leite, M.H., Boivin, V. and Corthésy, R. (2010), "Stress calculation methods for overcoring techniques in heterogeneous rocks", *Int. J. Rock Mech. Min. Sci.*, **47**(7), 1180-1192.
- ASTM E837 - 08e1 (2008), "Standard Test Method for Determining Residual Stresses by the Hole-Drilling Strain-Gage Method", ASTM International, West Conshohocken, PA, DOI: 10.1520/E0837-08E01.
- Barrallo, J., Zulueta, A. and Sánchez-Beitia, S. (1999), "The donostia method for the stress measurements in architectural heritage", *Strain*, **35**(3), 107-112.

- Sánchez-Beitia, S. (2007), “Stress analysis in the Altes Museum (Berlin) by means of the Hole Drilling Technique (Donostia Method)”, *Construct. Build. Mater.*, **21**(8), 1680-1688.
- Sánchez Beitia, S. (2008), “Stress analysis of the piers of the Tarazona Cathedral (Zaragoza-Spain) by means of the hole-drilling technique”, *Construct. Build. Mater.*, **22**(5), 966-971.
- Sánchez-Beitia, S. and Shueremans, L. (2009), “The Hole Drilling technique for on site deduction of the stresses states in stone masonry by using eight strain gages”, *Construct. Build. Mater.*, **23**, 2041-2046.
- McGinnis, M.J., Pessiki, S. and Turker, H. (2005), “Application of 3D digital image correlation to the core-drilling method”, *Exper. Mech.*, **45**(4), 359-367.
- Trautner, C., McGinnis, M.J. and Pessiki, S. (2011), “Application of the incremental core-drilling method to determine in-situ stresses in concrete”, *ACI Mater. J.*, **108**(3), 290-299.
- Coetzer, S. (1997), “Conceptual development of a method to determine the principal stress around coal mine workings to ensure safe mine design”, Final Project Report, Safety in Mines Research Advisor Committee (SIMRAC).
- Zhu, L., Xu, Q., Li, X. and Zhu, C. (2010), “Experimental studies of reinforced concrete column capacity affected by core drilling”, *Adv. Mater. Res.*, **133-134**, 1195-1200.
- Campione, G. and Minafò, G. (2011), “Experimental investigation on compressive behavior of bottle-shaped struts”, *ACI Struct. J.*, **108**(3), 294-303.
- ASTM C 1196 (2009), “Standard test method for in situ compressive stress within solid unit masonry estimated using flatjack measurements”, ASTM International, West Conshohocken, PA, DOI: 10.1520/C1196-09.
- Cervenka, V. (2000), “Simulating a response”, *Concrete Eng. Int.*, **4**(4), 45-49.
- ACI Committee 318 (2008), “Building code requirements for structural concrete (ACI 318-08)”, and Commentary (ACI 318R-08), American Concrete Institute, Detroit, Michigan.
- Eurocode 2, “Design of concrete structures - Part 1-1: General - Common rules for building and civil engineering structures”.

Notations

- A_s = total area of longitudinal bars
- A_{sw} = total area of stirrups
- b = side of the cross-section of the specimen
- E_{cm} = modulus of elasticity of concrete
- f_c = cylinder compressive strength of concrete
- f_{cm} = average cylinder compressive strength of concrete
- f_y = yield stress of steel reinforcements
- f_u = ultimate stress of steel reinforcements
- h = height of the cross-section of the specimen
- p = spacing between two successive stirrups
- R_c = cube compressive strength of concrete
- ε_x = vertical strain in the specimen
- ε_x = horizontal strain in the specimen
- ε_u = ultimate strain of steel reinforcements
- ν = Poisson's coefficient of concrete
- ρ = $A_s/(b \times h)$ = geometrical ratio for longitudinal bars
- ρ_{sw} = $A_{sw}/(p \times h)$ = geometrical ratio of stirrups in the pitch p
- σ_{xx} = principal stress in x-direction in the specimen
- σ_{yy} = principal stress in y-direction in the specimen